A Critical Role for Muscle Ring Finger-1 in Acute Lung Injury–associated Skeletal Muscle Wasting

D. Clark Files[1,2], Franco R. D'Alessio[1], Laura F. Johnston[1], Priya Kesari[1], Neil R. Aggarwal[1], Brian T. Garibaldi[1], Jason R. Mock[1], Jessica L. Simmers[3], Antonio DeGorordo[1], Jared Murdoch[1], Monte S. Willis[4], Cam Patterson[4], Clarke G. Tankersley[5], Maria L. Messi[6], Chun Liu[2], Osvaldo Delbono[6], J. David Furlow[7,8], Sue C. Bodine[7,8], Ronald D. Cohn[3], Landon S. King[1], and Michael T. Crow[1]

[1]Division of Pulmonary and Critical Care Medicine, Johns Hopkins Asthma and Allergy Center, Baltimore, Maryland; [3]McKusick-Nathans Institute of Genetic Medicine, Baltimore, Maryland; [4]McAllister Heart Institute, University of North Carolina, Chapel Hill, North Carolina; [5]Department of Environmental Health Sciences, School of Public Health, Johns Hopkins University, Baltimore, Maryland; [6]Department of Internal Medicine-Gerontology and [2]Internal Medicine-Pulmonary, Critical Care, Allergy and Immunology, Wake Forest University School of Medicine, Winston-Salem, North Carolina; and [7]Department of Neurobiology, Physiology, and Behavior, and [8]Department of Physiology and Membrane Biology, University of California, Davis, California

***Rationale*: Acute lung injury (ALI) is a debilitating condition associated with severe skeletal muscle weakness that persists in humans long after lung injury has resolved. The molecular mechanisms underlying this condition are unknown.**

***Objectives*: To identify the muscle-specific molecular mechanisms responsible for muscle wasting in a mouse model of ALI.**

***Methods*: Changes in skeletal muscle weight, fiber size, *in vivo* contractile performance, and expression of mRNAs and proteins encoding muscle atrophy–associated genes for muscle ring finger-1 (MuRF1) and atrogin1 were measured. Genetic inactivation of MuRF1 or electroporation-mediated transduction of miRNA-based short hairpin RNAs targeting either MuRF1 or atrogin1 were used to identify their role in ALI-associated skeletal muscle wasting.**

***Measurements and Main Results*: Mice with ALI developed profound muscle atrophy and preferential loss of muscle contractile proteins associated with reduced muscle function *in vivo*. Although mRNA expression of the muscle-specific ubiquitin ligases, MuRF1 and atrogin1, was increased in ALI mice, only MuRF1 protein levels were up-regulated. Consistent with these changes, suppression of MuRF1 by genetic or biochemical approaches prevented muscle fiber atrophy, whereas suppression of atrogin1 expression was without effect. Despite resolution of lung injury and down-regulation of MuRF1 and atrogin1, force generation in ALI mice remained suppressed.**

***Conclusions*: These data show that MuRF1 is responsible for mediating muscle atrophy that occurs during the period of active lung injury in ALI mice and that, as in humans, skeletal muscle dysfunction persists despite resolution of lung injury.**

AT A GLANCE COMMENTARY

Scientific Knowledge on the Subject

Muscle weakness contributes to the mortality and long-term morbidity of acute lung injury (ALI) in patients. There are currently no reported animal models of ALI-associated skeletal muscle wasting or established molecular mechanisms of how such wasting occurs.

What This Study Adds to the Field

We present a mouse model of ALI-associated skeletal muscle wasting that replicates many of the features of ALI-associated skeletal muscle wasting in humans and show that the muscle-specific E3 ubiquitin ligase, known as muscle ring finger-1, is a critical mediator of the ALI-associated skeletal muscle wasting that occurs in this model.

Keywords: skeletal muscle atrophy; intensive care unit–acquired weakness; critical illness myopathy; muscle atrophy genes; proteasomal-mediated protein degradation

Acute lung injury (ALI) is a syndrome characterized by the acute onset of pulmonary infiltrates and respiratory failure often leading to the need for mechanical ventilation (1). Approximately 200,000 people per year develop ALI in the United States, with mortality high at 30–40% (2). A common complication associated with ALI is skeletal muscle weakness. Weakness in these patients results in decreased long-term mobility and functional status. Skeletal muscle weakness is initiated early in the course of ALI, and has been shown to persist in a large percentage of patients for up to 5 years after resolution of lung injury and hospital discharge (3–6). Although multiple factors may contribute to ALI-induced muscle atrophy including reduced nutrition, inactivity caused by bed rest, and systemic inflammation, the etiology of ALI-associated skeletal muscle atrophy remains incompletely understood.

Skeletal muscle weakness is a common finding not only among patients with ALI, but also in patients with other critical illnesses. Clinically apparent weakness is present in 20–50% of patients with critical illness and has been shown to be an independent risk factor for mortality in these patients (3, 5, 7, 8). A variety of terms have been used in the literature to describe the myopathic weakness in these patients including acute quadriplegic myopathy, critical illness myopathy, and thick filament

(*Received in original form June 29, 2011; accepted in final form January 12, 2012*)

Supported by NIH NIAMS F32AR057637 (D.C.F.); NIH NHLBI HL089346 (L.S.K.); pilot grant (NIH P30 DK072488) (M.T.C.); AHA Biomedical Research Grant (M.T.C.); and Eudowood Foundation Bauernschmidt Fellowship Award (D.C.F.).

Author Contributions: D.C.F., F.R.D., L.S.K., and M.T.C. conceived and designed experiments; D.C.F., F.R.D., L.F.J., P.K., N.R.A., B.T.G., J.R.M., J.L.S., A.D., M.L.M., C.L., J.M., and O.D. performed experiments and analysis; M.S.W. and C.P. provided transgenic mice; J.D.F. and S.B. provided research reagents; C.G.T. and R.D.C. provided equipment and oversight for physiologic experiments; and D.C.F. and M.T.C. wrote the manuscript and provided creative input.

Correspondence and requests for reprints should be addressed to Michael T. Crow, Ph.D., Johns Hopkins University School of Medicine, Division of Pulmonary and Critical Care Medicine, The Johns Hopkins Asthma and Allergy Center, 5A.58, 5501 Hopkins Bayview Circle, Baltimore, MD 21224. E-mail: mcrow1@jhmi.edu

This article has an online supplement, which is accessible from this issue's table of contents at www.atsjournals.org

Am J Respir Crit Care Med Vol 185, Iss. 8, pp 825–834, Apr 15, 2012

Originally Published in Press as DOI: 10.1164/rccm.201106-1150OC on February 3, 2012
Internet address: www.atsjournals.org

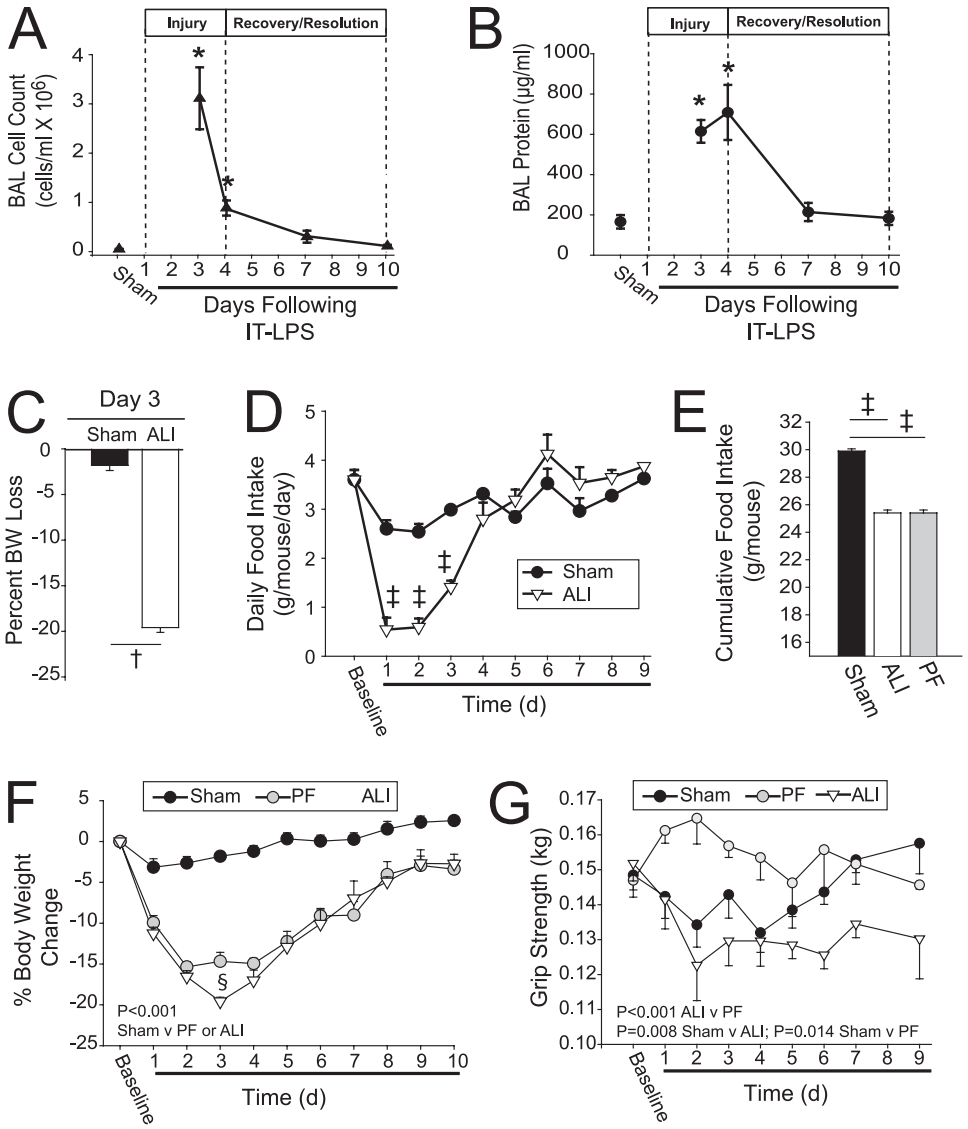

Figure 1. Acute lung injury (ALI) induces body weight loss, reduced food consumption, and muscle weakness. Bronchoalveolar lavage fluid (BALF) of ALI (intratracheal [IT]-LPS) and sham (IT-H_2O) mice revealed an increase in total cell count (*A*) and total protein (*B*) that peaked between Days 3 and 4 in ALI mice and returned to baseline by Day 10. $^{*}P < 0.03$ versus baseline values; n = 5–6. Based on these data and the accompanying histology of the lungs (*see* Figure E1), we refer to the period between Days 1 and 4 after IT-LPS as the "lung injury phase" and between Days 4 and 10 as the "lung resolution phase." (*C*) ALI mice have an approximate 20% drop in body weight (BW) 3 days after IT-LPS. $^{\dagger}P < 0.001$; n = 5. (*D*) Food consumption dramatically falls in ALI mice after IT-LPS (*open triangles*) compared with sham-operated mice (*black circles*). $^{\ddagger}P < 0.01$. (*E*) Pair-fed (PF) mice were used to control for the effects of reduced food consumption. These mice underwent a sham surgery (IT-H_2O) and had food intake matched to that consumed by ALI mice on a daily basis. The data in the bar graphs show that cumulative food intake over the 10 days of lung injury and resolution was equal in PF and ALI mice. $^{\ddagger}P < 0.01$. (*F*) Whole body weight loss profiles were similar in PF (*gray circles*) and ALI mice (*open triangles*) but significantly different from changes in the body weights of sham mice (*black circles*) (analysis of variance, $P < 0.001$ for group differences), except for Day 3. $^{\S}P < 0.03$; n = 5. (*G*) Despite similar body weight losses, ALI mice had reduced grip strength compared with PF mice (analysis of variance, $P < 0.001$). Data are expressed as means ± SEM. $^{*}P < 0.001$, ALI versus PF; $P = 0.008$, sham versus ALI; $P = 0.014$, sham versus PF. n = 8–10 in each group.

myopathy, the latter referring to the preferential loss of myosin observed in the muscles of these patients (9–11).

Studies over the last 12 years have defined important roles for muscle-specific genes that regulate muscle wasting in well-defined models of skeletal muscle atrophy, including immobilization, denervation, and hindlimb suspension (12). Prominent among these are the genes *Fbx032* (atrogin1 or MAFbx) and *Trim63* (muscle ring finger protein-1 [MuRF1]), both of which function as ubiquitin E3 ligases in the proteasome-mediated degradation of skeletal muscle proteins (12, 13). Up-regulation of MuRF1 and atrogin has also been observed in the peripheral muscles of patients with chronic obstructive pulmonary disease and in the diaphragms of mechanically ventilated brain-dead patients (14, 15).

In this study, we used a mouse model of ALI to define the molecular mechanisms responsible for ALI-induced muscle wasting. This model of direct lung injury is highly reproducible and proceeds through distinct injury and resolution phases over a relatively short time course (16). Our data show that there is a marked up-regulation of MuRF1 and atrogin1 gene expression in ALI mice within 2–3 days after inducing lung injury and, as in human ALI, contractile dysfunction triggered by ALI that persists despite down-regulation of MuRF1 and atrogin1 gene expression and complete resolution of lung injury. We tested the hypothesis that MuRF1 is necessary for the ALI-associated decrease in muscle mass and loss of contractile proteins during the period of active lung injury. Some of the results of these studies have been previously reported in abstract form (17–19).

METHODS

Animals

All animal experiments were conducted under protocols approved by the Johns Hopkins Animal Care and Use Committee. Eight-week-old male C57BL/6 mice (The Jackson Laboratory, Bar Harbor, ME) were housed in a pathogen-free facility. To induce lung injury, mice were anesthetized with an intraperitoneal (IP) injection of 150 mg/kg ketamine and 13.5 mg/kg acetylpromazine and the trachea exposed. *Escherichia coli* LPS (O55:B5 L2880; Sigma-Aldrich, St. Louis, MO) at 3 μg/g mouse or an equivalent volume of sterile H_2O (sham control) was then instilled intratracheally using a 20-gauge catheter. Animals were not mechanically ventilated and oxygenation or activity levels were not monitored. For IP-LPS studies, mice were given 3 μg/g LPS IP and harvested at subsequent time points. Breeding pairs of MuRF1$^{+/-}$ mice were provided by Drs. Cam Patterson and Monte

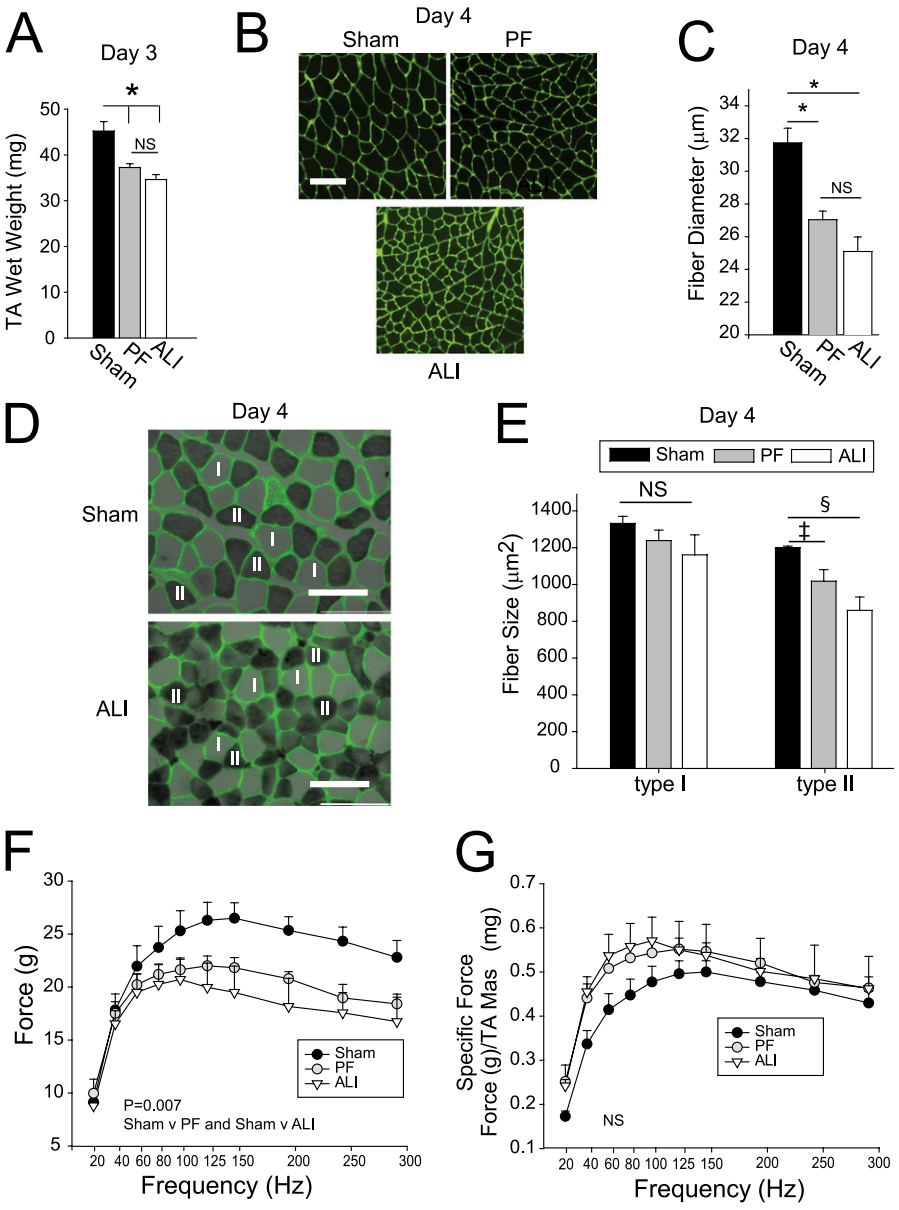

Figure 2. Acute lung injury (ALI) and pair-fed (PF) mice develop skeletal muscle atrophy. (*A*) Tibialis anterior (TA) muscle wet weights were decreased in PF and ALI mice by Day 3 post–intratracheal (IT)-LPS. $*P < 0.003$; n = 6. (*B*) Cross-sections of TA muscles from sham, ALI, and PF mice at Day 4 post–IT-LPS. Muscle fibers were identified by sarcolemmal staining for γ-laminin. Scale bar = 100 μm. (*C*) Mean fiber diameters of sham, PF, and ALI from Day 4 mice. $*P < 0.003$; n = 5. (*D*) Combined myosin ATPase histochemistry (alkaline preincubation) and γ-laminin staining enabled independent fiber size measurements of type I (*light staining*) and type II (*dark staining*) muscle fibers in the soleus. (*E*) Summary of mean muscle fiber diameters segregated by experimental group and muscle fiber type. Data are expressed as means ± SEM. $^{\S}P < 0.03$; $^{\ddagger}P < 0.02$. Scale bar as in (*B*). (*F*) Force-frequency curves for Day 4 sham, PF, and ALI hindlimb muscles showing reduced contractile force production in PF and ALI mice. (*G*) Specific force–frequency curves for Day 4 sham, PF, and ALI mice. Normalization of force to muscle mass for all three groups shows no difference in contractile performance.

Willis of the McAllister Heart Institute at the University of North Carolina.

Bronchoalveolar Lavage and Analysis

At specified times after instillation, mice were anesthetized, blood or bronchoalveolar lavage fluid (BALF) removed, and the animals then killed by exsanguination. BALF counts and protein analyses were performed as previously described (16).

Lung Histology

Lungs were inflated to 25 cm H_2O with 1% low-melting agarose (Invitrogen, San Diego, CA); fixed in 10% formalin; then embedded in paraffin and sectioned for histologic evaluation by hematoxylin and eosin staining (20).

Measurement of Plasma Levels of LPS

Blood was collected retroorbitally from mice at 6, 24, and 72 hours after intratracheal (IT) H_2O, IT-LPS, or IP-LPS administration and then placed in ethylenediaminetetraacetic acid–coated tubes. Mice were then killed by administration of ketamine and acepromazine followed by cervical dislocation. The blood was prepared for measurements of LPS (Limulus assay) levels, according to the manufacturer's instructions (Hycult Biotech, Plymouth Meeting, PA).

Mouse Grip Strength

Mouse grip strength was measured using a grip strength meter (Columbus Instruments, Columbus, OH) and the peak force generated from one of five successive trials was recorded as described previously (21).

Statistical Evaluation of Data

Data are expressed as the mean ± SEM or median and interquartile ranges. Unpaired Student *t* test, analysis of variance, or the Mann-Whitney test was used for statistical comparisons when appropriate. Differences were considered significant at P less than 0.05.

Additional methods for reverse transcriptase quantitative polymerase chain reaction, Western blotting, *in vivo* force measurements, plasmid generation, and skeletal muscle electroporation are provided in the online supplement.

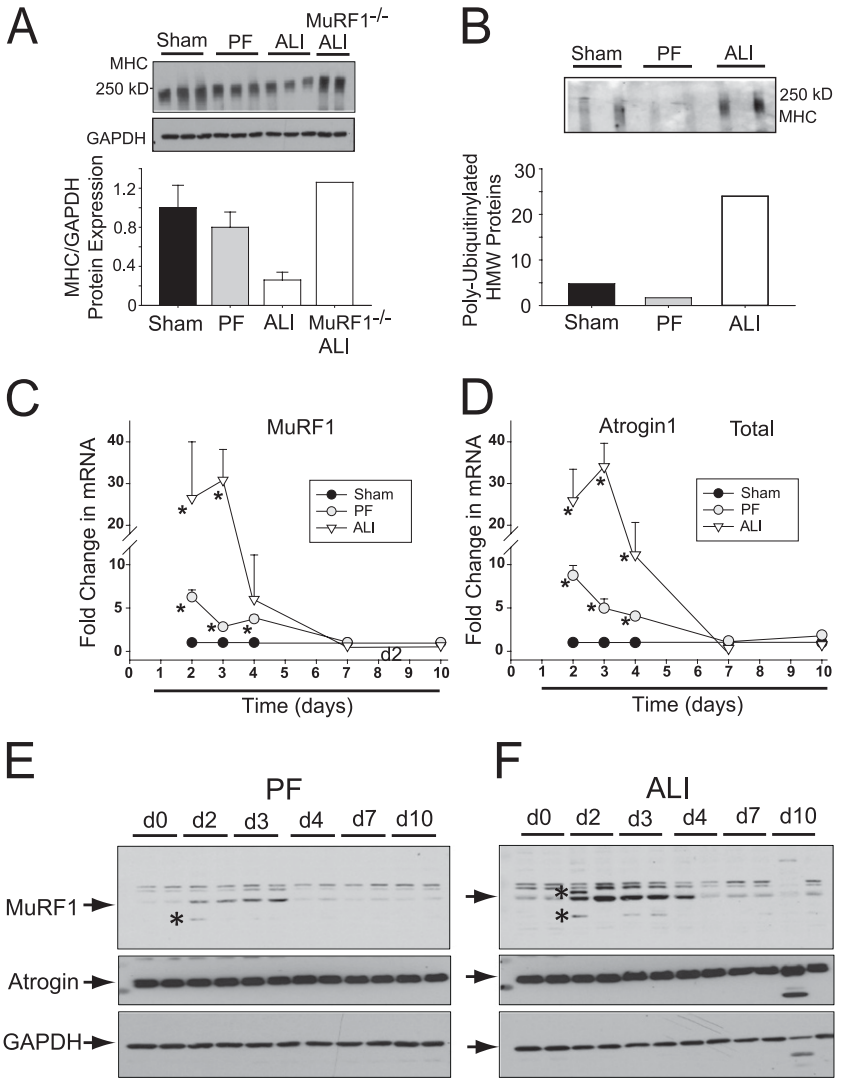

Figure 3. Myosin heavy chain (MHC) degradation, ubiquitination, and increased muscle atrogene expression in pair-fed (PF) and acute lung injury (ALI) mice. (*A*) Western blots showing sarcomeric MHC abundance in sham, PF, and ALI mice and MHC from ALI muscle ring finger-1 (MuRF1)$^{-/-}$ mice (*top*). Quantification of expression normalized to glyceraldehyde phosphate dehydrogenase (GAPDH) expression (*bottom*). (*B*) Western blot of extracts from sham, PF, and ALI muscles show a marked increase in high molecular weight (HMW) polyubiquinated proteins (*top*). Quantification of expression expressed in arbitrary units (*bottom*). Results of quantitative reverse transcriptase polymerase chain reaction measurements of MuRF1 (*C*) and atrogin1 (*D*) mRNA expression in muscles from PF and ALI mice versus expression in sham mice. *$P < 0.02$; n = 5–8. (*E* and *F*) Time course of MuRF1 and atrogin1 protein expression in PF and ALI mice. PF mice exhibit a relatively weak expression of MuRF1 proteins, whereas up-regulation of MuRF1 protein in ALI is much stronger. Neither PF nor ALI muscles exhibit any change in atrogin1 protein levels at any time and under any condition tested. *Possible processing intermediates of MuRF1.

RESULTS

IT-LPS Causes ALI and Reduced Muscle Function

As described previously (16, 22, 23) and shown in Figure E1 in the online supplement, IT-LPS induced within 3 days a pattern of lung injury that was distinguished by severe alveolar consolidation with cellular infiltrates and interstitial thickening. At 7 days post–IT-LPS, lung injury had nearly resolved, and by Day 10 the lungs appeared normal. Total BALF cell counts and protein levels (Figures 1A and 1B) followed a similar time course, rising during the period of active lung injury (Days 1–4) and returning to baseline during the lung recovery and resolution phases (Days 5–10). Sham mice receiving IT-H_2O and then killed at Day 3 showed no evidence of lung injury (sham data points, Figures 1A and 1B). Data in the literature and experiments described in Figure E2 suggest that this IT-LPS model differs significantly in its pharmacokinetics from IP-LPS models of sepsis (22, 23).

Within 3 days after the administration of IT-LPS to mice (hereafter referred to as ALI mice), there was an approximate 20% loss in body weight (Figure 1C). Because loss of body weight could be caused in part or in whole by the marked reduction in food intake by ALI mice (Figure 1D), we generated pair-fed (PF) mice to control for this effect (Figure 1E). Importantly, despite similar weight loss profiles in PF and ALI mice (Figure 1F), only ALI mice exhibited a significant drop in muscle force production as measured by a grip strength meter (Figure 1G).

Reduced Muscle Function Is Associated with Skeletal Muscle Atrophy

To assess muscle atrophy in sham, PF, and ALI mice in response to lung injury, we first measured the wet weights of the tibialis anterior (TA) muscles. TA wet weights in PF and ALI mice were significantly lower than in sham mice (Figure 2A). To elucidate the mechanisms underlying these losses, we measured the size distribution of muscle fibers sorted by diameter as described in the online supplement. Figure 2B shows images of cryosections with the sarcolemmae delineated by γ-laminin immunofluorescence chemistry. Figure E3 shows a histogram of the size distribution of fiber diameters and Figure 2C the mean fiber diameters from each of the three groups. These data reveal that mean fiber diameters of ALI and PF mice were statistically different from time-matched controls but not from each other (Figures 2B and 2C).

To determine if different muscle fibers are differentially affected by ALI, mean fiber diameters of types I and II muscle fibers were assessed using the soleus muscle, because the TA muscle has few type I fibers. Staining of the muscles to identify type I (*light*

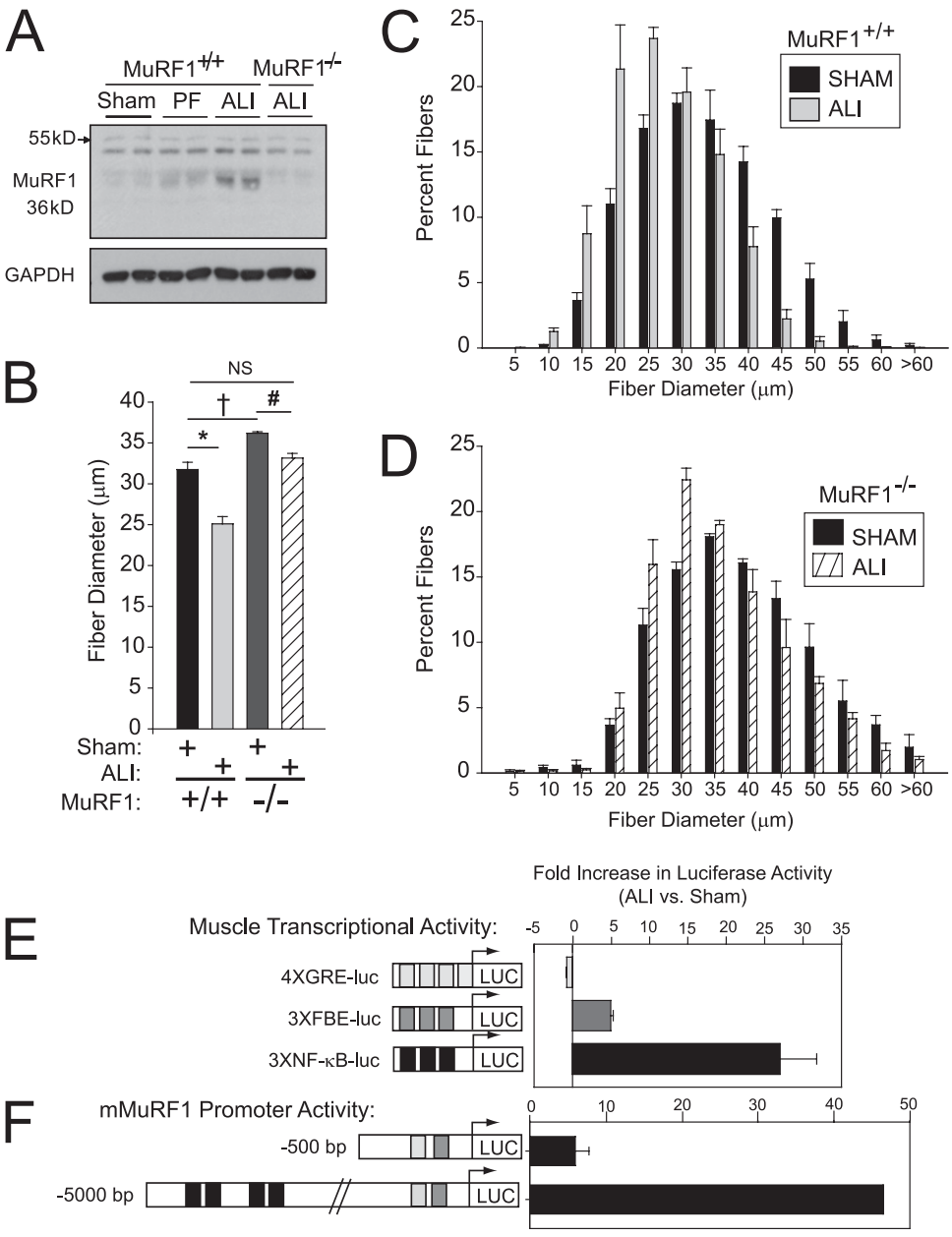

Figure 4. Muscle wasting in muscle ring finger-1 (MuRF1)$^{-/-}$ mice and increased nuclear factor (NF)-κB activity in acute lung injury (ALI) wild-type (WT) mouse muscles. (*A*) Western blot of MuRF1 protein expression shows up-regulation in ALI MuRF1 WT but no up-regulation in ALI MuRF1$^{-/-}$ mouse muscles. GAPDH = glyceraldehyde phosphate dehydrogenase; PF = pair fed. (*B*) Mean fiber diameters for WT and MuRF1$^{-/-}$ tibialis anterior (TA) muscles show a moderate increase in mean muscle fiber diameters in sham control MuRF1$^{-/-}$ mice. Exposure to ALI markedly reduces mean muscle fiber diameter in WT muscles mice but only a slight reduction in the MuRF1$^{-/-}$ muscle. *$P = 0.004$; †$P = 0.007$; #$P = 0.03$. (*C*) Histograms of the fiber distribution of sham and ALI-treated MuRF1$^{+/+}$ (WT) muscles reveal a large shift to the left (*smaller size*). (*D*) Histograms of the fiber distribution of sham and ALI-treated MuRF1$^{-/-}$ (knockout) muscles show only a small shift to the left and smaller fiber diameters. (*E*) Assessment of ALI-induced muscle transcriptional activity was measured by electroporating plasmids in which firefly luciferase transcription was controlled by transcriptional response elements specific for glucorticoid signaling (4XGRE-luc), FOXO signaling (3XFBE-luc), and NF-κB signaling (3XNf-κB-luc). Only increases in FBE- and NF-κB–luciferase activity is significantly up-regulated in ALI. (*F*) Luciferase reporter for MuRF1 transcriptional activity containing either no NF-κB binding elements (500 MuRF1-luc) or multiple NF-κB binding sites (5,000 MuRF-luc).

gray) and II (*dark gray*) fibers is shown in Figure 2D and the mean fiber distribution of types I and II fibers is summarized in Figure 2E. The results show that type II muscle fibers are differentially affected by ALI-induced muscle wasting.

Because grip strength measurements reflect not only the contractile properties of the muscle, but also neurogenic and behavioral effects, we also measured muscle force production elicited by *in situ* stimulation of the peritoneal nerve. Day 4 PF and ALI mice showed a similar reduction in absolute force generation compared with sham mice (Figure 2F). Specific force generation (absolute force normalized to muscle mass), however, was the same for all three groups (Figure 2G), suggesting that decreased force generation in ALI and PF mice at Day 4 may be directly caused by loss of muscle mass alone (Figure 2A).

MuRF1 Protein Levels Are Differentially Regulated in ALI and PF Mice

Although loss of muscle mass and mean fiber diameter were similar in PF and ALI mice during the period of active lung injury (Days 2–4), an analysis of the molecular changes occurring in these mice revealed substantial qualitative differences. Figure 3A shows that the expression of sarcomeric muscle myosin heavy chain (MHC) proteins was suppressed in PF mice and even more so in ALI mice. Because striated MHCs are well-described targets for degradation by the ubiquitin-proteasomal system (24), we measured levels of polyubiquinated proteins in the three experimental groups (Figure 3B) and found that they were increased in ALI but not PF mice. The blot in Figure 3B shows extensive ubiquitination of proteins coincident with sarcomeric MHCs.

Two of the most common genes up-regulated in muscle wasting are *Trim63* (MuRF1) and *Fbxo32* (atrogin1) (12, 13, 25–27). These proteins function as muscle-specific ubiquitin E3-ligases that tag proteins for the ubiquitin-proteasomal pathway. Figures 3C and 3D show that MuRF1 and atrogin1 mRNA expression were markedly up-regulated in the TA muscles of ALI mice, but only modestly up-regulated in PF muscles. Expression of MuRF1 protein followed a pattern similar to its mRNA, higher in ALI muscles (Figure 3F) and lower in PF muscles (Figure 3E), whereas the expression of

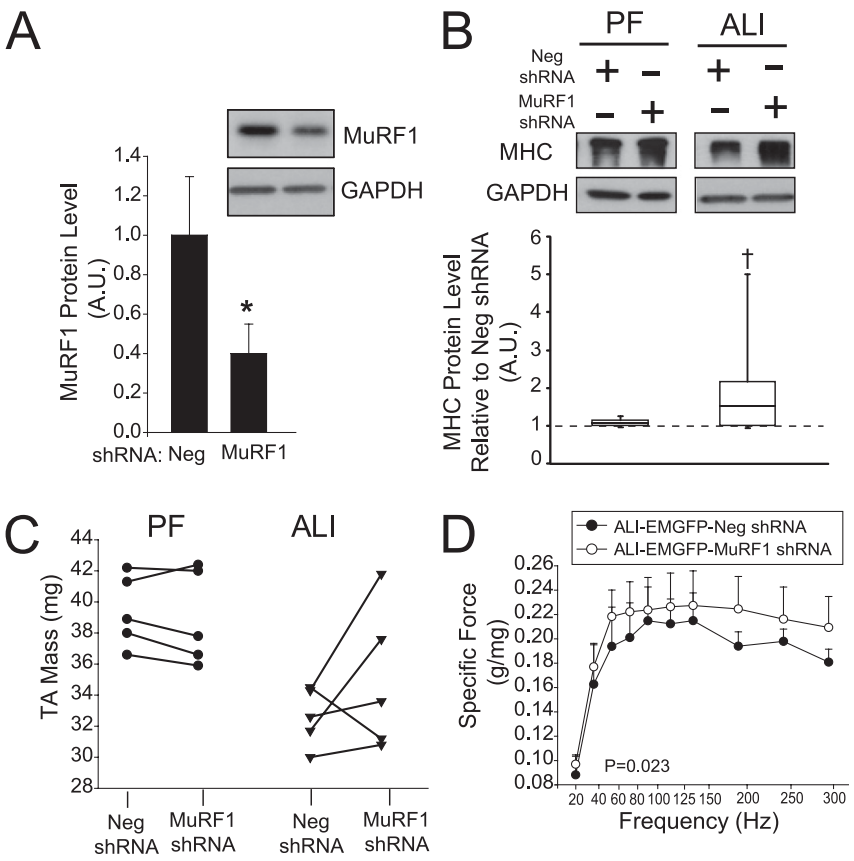

Figure 5. Muscle ring finger-1 (MuRF1) miRNA-based short hairpin (sh) RNAs effectively blocks MuRF1 protein expression in pair-fed (PF) and acute lung injury (ALI) mice but increases myosin heavy chain (MHC) content only in acute lung injury (ALI) mice. (*A*) Immunoblots of MuRF1 and glyceraldehyde phosphate dehydrogenase (GAPDH) from muscles transduced with Emerald GFP (EmGFP)-Neg control (NEG) shRNA or EmGFP-MuRF1 shRNA show that MuRF1 expression is reduced by approximately 70% in MuRF1 shRNA muscles. $^{*}P < 0.008$. (*B*) Knockdown of MuRF1 protein by the EmGFP-MuRF1shRNA plasmid increased MHC content in ALI mice but had no effect on MHC levels in PF mice. *Dotted line* in *B* represents MHC level in control (EmGFP-Neg shRNA) muscles. $^{\dagger}P = 0.03$. (*C*) Differences in tibialis anterior (TA) muscle mass in muscle transduced with EmGFP-MuRF1 shRNA, with results expressed with reference to EmGFP-Neg shRNA. (*D*) *In situ* force–frequency curves for muscles transduced with EmGFP-Neg and EmGFP-MuRF shRNAs and analyzed at Day 10. Data show an increase in force production by MuRF1 shRNA versus NEG shRNA. $P = 0.023$.

atrogin1 protein was not affected by any condition. Data in Figure E4 show that MuRF1 and atrogin1 mRNA expression were also up-regulated in the diaphragms from Day 3 ALI mice.

MuRF1 Is Necessary for Skeletal Muscle Wasting during the Period of ALI

Because the previously mentioned data reveal a strong association of MuRF1 mRNA and protein expression with ALI-associated skeletal muscle wasting, we tested MuRF1's role in ALI-associated muscle wasting in MuRF1$^{-/-}$ (knockout [KO]) mice. We probed muscle extracts from sham, PF, and ALI wild-type (WT) mice and ALI KO mice and found, as expected, that MuRF1 expression increased only in ALI WT mice (Figure 4A). The mean fiber diameter of the TA muscle in untreated MuRF1 KO mice at baseline was slightly larger than in untreated WT mice (Figure 4B). Although ALI resulted in a reduction of the mean fiber diameter of greater than 25% in WT mice, the reduction in mean muscle fiber diameter in MuRF1 KO ALI mice was less than 5% and not significantly different from the mean muscle fiber diameter in untreated WT mice. These data show that the up-regulation of MuRF1 is required for ALI-induced skeletal muscle wasting.

We then searched for signaling pathways that are preferentially activated during lung injury and capable of driving increased MuRF1 transcription in ALI muscles. Other studies have implicated signaling through glucocorticoid receptors, FOXO proteins, and nuclear factor-κB (NF-κB) transcriptional activity as important regulators of muscle wasting (28–31). We introduced plasmids reporting on each of these pathways into TA muscles and assessed their activity 3 days after either sham or ALI treatment. The data in Figure 4E show that reporter activity for glucocorticoid signaling (4XGRE-luc) was not up-regulated in ALI mice, whereas FOXO (3XFBE-luc) and NF-κB (3XNF-κB-luc) signaling were increased by more than 5- and 25-fold, respectively. To determine if the marked up-regulation of NF-κB activity in ALI mice was linked to MuRF1 gene transcription, we compared the ALI-induced activation of two different MuRF1 promoter constructs, one lacking the all NF-κB binding sites (−500 MuRF1) and the other containing multiple NF-κB sites (−5,000 MuRF1). The data in Figure 4F show that the 5,000 MuRF1 reporter construct was activated nearly 50-fold in ALI muscles, more than 10 times that of the 500 MuRF1 reporter. These results show that NF-κB activity is markedly and selectively up-regulated in ALI muscles and that this up-regulation drives increased MuRF1 transcription.

Suppression of Muscle Wasting in ALI Mice by Plasmid-based shRNAs

To control for potential developmental effects of congenitally decreased MuRF1 expression in MuRF1 KO mice, we also transduced plasmids coexpressing Emerald GFP (EmGFP) and miRNA-based short hairpin (sh) RNAs directly into TA muscles by electroporation. Figures E5 and E6 show the relative effectiveness of these shRNAs in cells expressing mouse MuRF1 or atrogin, respectively. One week later, the mice were randomly assigned to sham, PF, or ALI treatment groups and the muscles harvested 4 days later for analysis. From EmGFP expression, we determined that 70–80% of the muscle fibers in the mouse TA were transduced using our modification of the muscle electroporation technique (*see* Figure E7). Biochemical analyses of the entire muscle revealed an approximate 70% reduction in MuRF1 protein levels in MuRF1 shRNA-transduced muscles compared with muscles transduced with the EmGFP and a negative control shRNA (Figure 5A). With an overall *in vivo* transduction efficiency of 70–80%, MuRF1 protein levels in MuRF1 shRNA-transduced muscle fibers should be reduced by approximately 75–85%.

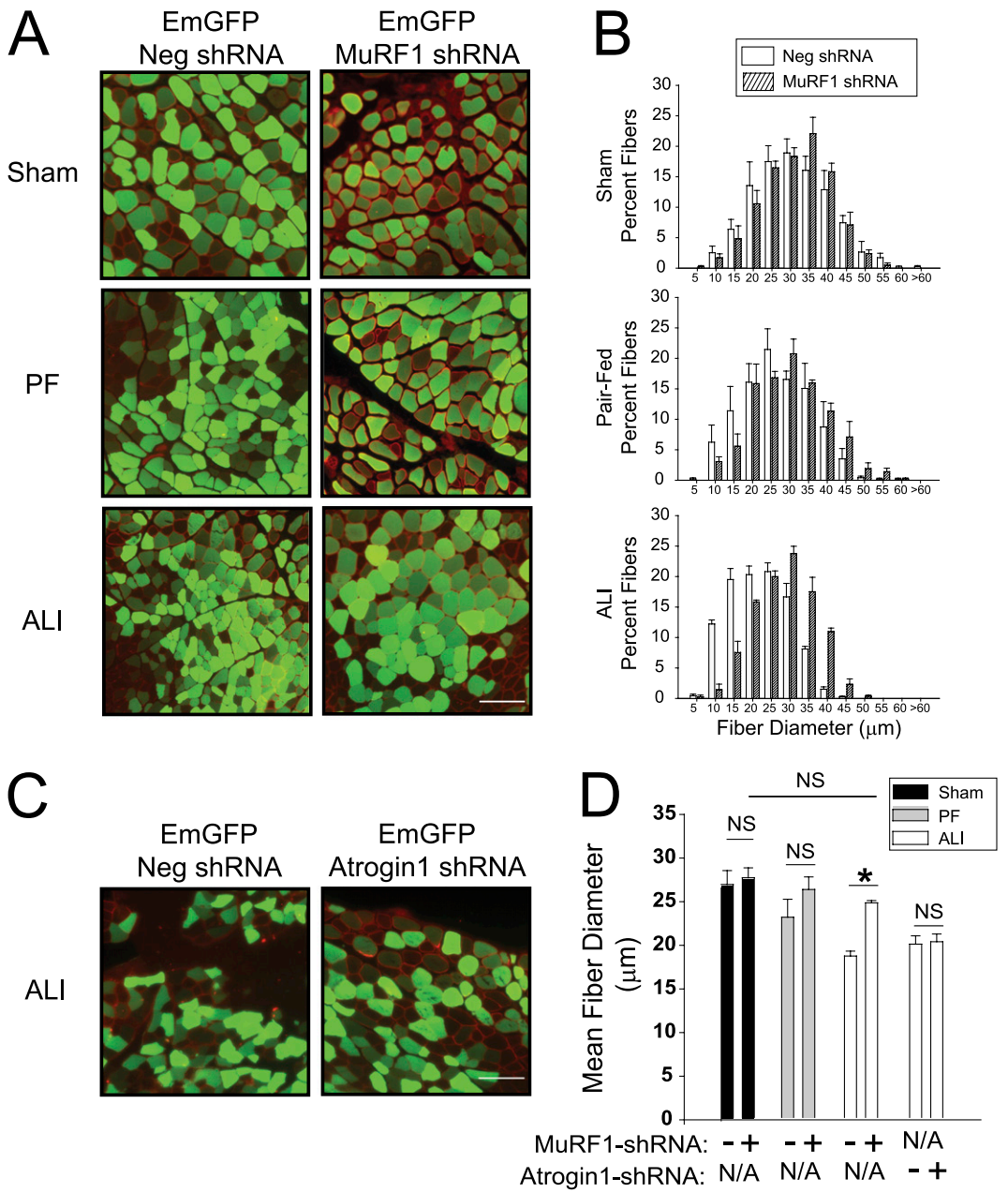

Figure 6. Muscle ring finger-1 (MuRF1) regulates muscle atrophy in acute lung injury (ALI) mice. Emerald GFP (EmGFP)-Neg shRNA or EmGFP-MuRF1 shRNAs were electroporated into the tibialis anterior (TA) muscles. One week later, mice underwent sham, pair-fed (PF), or ALI treatments. (*A*) Muscles were fixed at harvest and the sarcolemma stained with an antibody to dystrophin (*red*) to measure diameters of fibers expressing EmGFP. Scale = 100 μM. (*B*) Fiber histograms of sham, PF, and ALI mice treated with EMGFP-MuRF1 shRNA or EmGFP-Neg shRNAs. (*C*) The same technique was used to electroporate EmGFP-atrogin1 shRNA into the TA of ALI mice. (*D*) Mean fiber diameters of sham, PF, and ALI mice treated with MuRF1 or atrogin1 shRNAs. Fiber diameter is restored to sham conditions in ALI mice treated with MuRF1 shRNA but not atrogin1 shRNA. Data are expressed as means ± SEM. *$P < 0.006$; n = 5 in each group.

Using this approach, we found that the MuRF1 shRNA 520 effectively prevented muscle wasting in ALI muscles. First, we found that MuRF1 shRNA treatment in ALI mice significantly increased MHC expression but had no effect on MHC expression in PF mice (Figure 5B). In four out of five ALI mice, treatment with MuRF1 shRNA showed a trend toward increased TA muscle weight compared with the contralateral (Neg-shRNA) limb. In PF mice, the trend was toward a decrease in muscle weight with MuRF1 shRNA (Figure 5C). We also measured force production in ALI-MuRF1 shRNA and ALI-Neg shRNA mice. Although we found no change in force production at Day 4 post–IT-LPS (data not shown), we did observe a modest but significant restoration of force production with MuRF1 shRNA at Day 10 post–IT-LPS (Figure 5D). In addition, although the mean diameter of EmGFP-positive muscle fibers was unaffected in MuRF1 shRNA transduced muscles from sham and PF mice, there was a large rightward shift in fiber size distribution (increased muscle fiber diameter) and a statistically significant increase in mean fiber diameter in MuRF1 shRNA transduced muscles from ALI mice (Figures 6A, 6B, and 6D). We repeated this series of experiments using a second MuRF1 shRNA (610; *see* Figure E5) targeting a different region of the mouse MuRF1 coding sequence and obtained near-identical results.

We also constructed two plasmids encoding EmGFP and one of two atrogin1 shRNAs (384 and 534), which were transduced into the TA muscles of ALI mice (*see* Figure E6). In contrast to the results seen with the MuRF1 knockdown, however, knockdown of atrogin1 had no effect on ALI-associated muscle atrophy (Figures 6C and 6D). Together, these results show that inhibition of MuRF1, but not atrogin1, abrogates muscle fiber atrophy in ALI mice.

ALI Muscle Wasting Persists Despite Resolution of Lung Injury

Although data presented in Figures 1A and 1B and Figures E1 and E2 show that lungs are fully recovered from ALI by Day 10, mean fiber diameters in PF and ALI remained suppressed

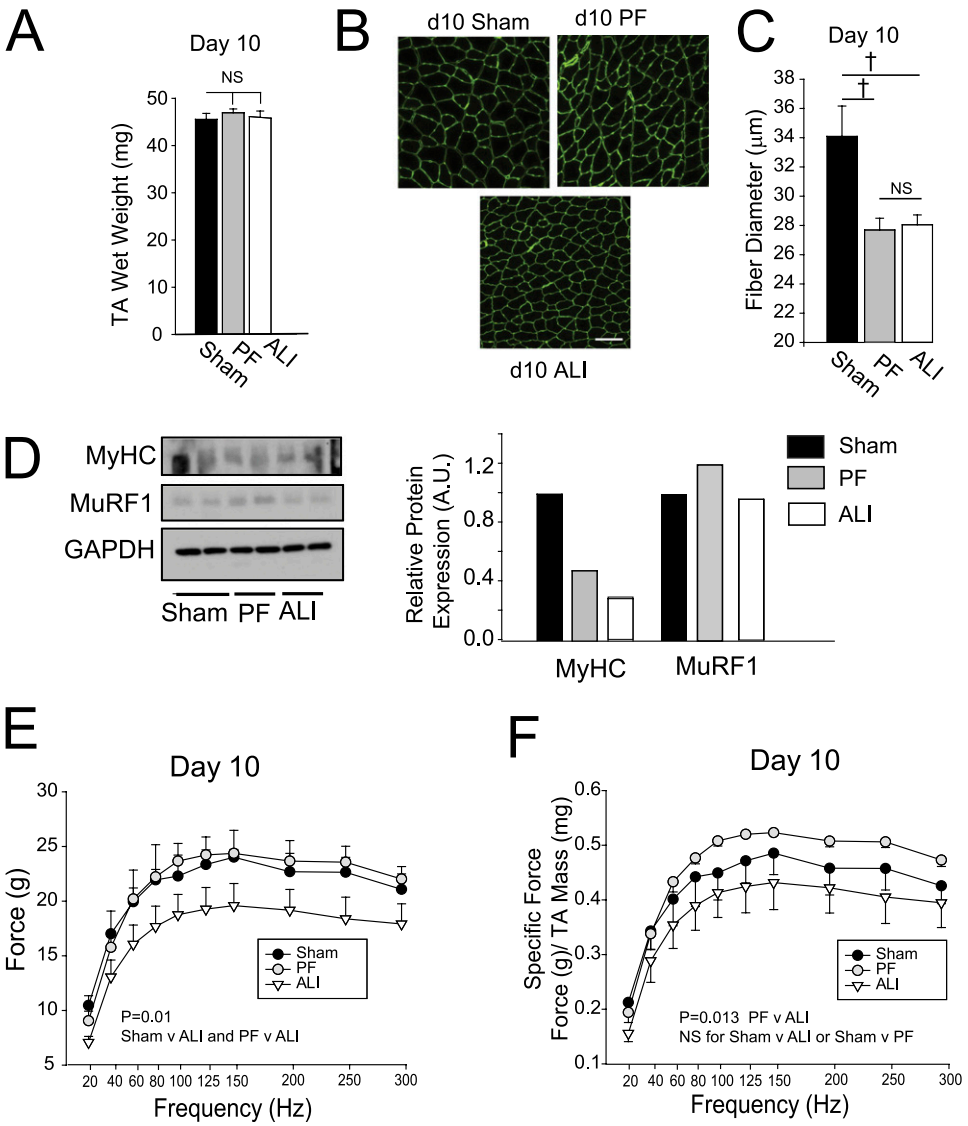

Figure 7. Persistence of muscle loss after complete resolution of lung injury. (*A*) Tibialis anterior (TA) wet weights at Day 10 in sham, pair-fed (PF), and acute lung injury (ALI) TA muscles are not significantly different. (*B*) Cryosections of γ-laminin–stained muscle sections from Day 10 sham, PF, and ALI mice. (*C*) Mean muscle fiber analysis of Day 10 muscles shows similar reductions in PF and ALI diameters compared with sham controls. $^{\dagger}P < 0.001$; n = 5. (*D*) Representative Western blots of myosin heavy chain (MyHC) and muscle ring finger-1 (MuRF1) protein expression shows that MyHCs remain reduced at Day 10, whereas MuRF1 protein expression is reduced in all groups (Figures 3E and 3F show a time course of MuRF1 protein expression from Days 0–10). GAPDH = glyceraldehyde phosphate dehydrogenase. (*E*) Force–frequency curves for Day 10 muscles show that ALI sham and PF curves are not significantly different for each other but are both significantly different from ALI muscle ($P = 0.01$). (*F*) Specific force–frequency curves at Day 10 show a significant difference between PF and ALI muscles ($P = 0.013$).

(Figures 7B and 7C). Wet weights of the PF and ALI muscles were, however, similar to sham control levels (Figure 7A). Although data in Figures 3E and Figure 7D show that Day 10 MuRF1 protein levels have been at baseline for several days, MHC protein levels remain depressed (Figure 7D). Absolute force production from the TA at Day 10 is similar in sham and PF mice, whereas force production in ALI mice is markedly suppressed (Figure 7E). When force measurements are normalized to muscle weight (specific force), the differences between PF and ALI persisted (Figure 7F). These data show that recovery of skeletal muscles from ALI is markedly delayed or suppressed despite complete resolution of lung injury and the down-regulation of MuRF1 mRNA and protein expression. They also show that the restoration of muscle mass alone (Figure 7A) is not sufficient to restore muscle function, evoking the possibility of intrinsic changes to the contractile apparatus, the latter consistent with the low levels of MHC expression in ALI mice at Day 10.

DISCUSSION

It is increasingly recognized that ALI-associated skeletal muscle wasting represents a clinically significant complication that contributes to the morbidity and mortality of ALI (3–5). Understanding the molecular mechanisms that promote and control skeletal muscle wasting associated with ALI is essential in designing therapeutic approaches targeting this syndrome. As an important step in that direction, we describe here a mouse model of ALI that displays some of the key features of human ALI-associated muscle wasting. These include skeletal muscle atrophy and weakness that is temporally tied to lung injury and the persistence of muscle weakness after resolution of lung injury, the later documented to be present in a large percentage of patients at least 5 years posthospitalization (3–6).

In our study, we show that there is a significant reduction in skeletal muscle mass within days of exposure of mice to IT-LPS that is associated with increased MuRF1 mRNA and protein expression. This reduction occurs selectively in type II fibers, consistent with the results of others (32). These changes are associated with high levels of NF-κB activity in ALI muscles (Figures 4E and 4F), which others have shown to be important in promoting muscle wasting associated with tumor cachexia (29) or denervation (27). Finally, we show that ALI-associated muscle wasting in mice is markedly suppressed in MuRF1-deficient but not atrogin-deficient muscles (Figures 4A–4D and 6A–6C). Importantly, our data also show that muscle weakness persists (Figures 7B–7F) despite resolution of lung injury and the return of atrophy-associated mRNAs and proteins to basal levels (Figures 3C–3F). These

changes are associated with reductions in the intrinsic contractility of the muscles (Figure 7F) and persistent suppression of striated muscle MHCs (Figure 7D).

The biochemical pathways most likely responsible for ALI-associated muscle wasting are the ubiquitin-mediated proteasomal and autophagy-lysosomal pathways. In our model, we uncovered evidence that both pathways were activated, the former shown in this report to be triggered by increased expression and activity of the muscle-specific E3 ligase, MuRF1, and the latter presumably by the marked reduction in food intake in ALI mice that triggered the up-regulation of selective autophagy-associated genes (33) and the need to include PF controls in the protocol (*see* Figure E10).

The use of PF controls is a common practice in the study of muscle-wasting disorders in which appetite is suppressed or access to food is limited. It is based on the assumption that the effects of reduced food intake on muscle mass and function are a separate, independent, and indirect component of the overall reduction in muscle mass caused by catabolic processes, such as the activation of the ubiquitin-mediated proteasomal pathway. If muscle wasting in ALI mice is a composite response of the effects of activating both proteasomal- and autophagy-mediated molecular and cellular degradation, then muscle wasting should be greater in ALI compared with PF muscle. Contrary to that prediction, our data show that muscle loss and reduction in muscle fiber diameters were similar in ALI and PF mice (Figures 2A, 2C, and 4B; *see* Figures E3, E8, and E9). Furthermore, suppressing MuRF1 expression through genetic inactivation or biochemical suppression in this model prevented the loss of muscle mass in ALI mice but had no effect in restoring muscle mass in PF muscles. These data show that all of the muscle wasting in ALI mice and none of it in PF mice was caused by increased MuRF1-driven proteasomal activity, excluding a direct contribution of autophagy to muscle wasting in ALI mice. These data are not consistent with the assumption that the secondary effects of pair-feeding are additive with the primary effects of ubiquitin-mediated proteolysis in muscle, but instead suggest that they may be interdependent and that crosstalk between the two degradative pathways decides which catabolic pathways are activated or suppressed. One likely candidate that might mediate this crosstalk is the protein p62 (sequestosome1) (34), which is a negative regulator of autophagy and a potential binding partner of MuRF1 (35).

In summary, our data demonstrate that ALI in mice produces marked skeletal muscle wasting and dysfunction similar to that observed in patients with ALI. Muscle wasting and dysfunction in this model is associated with markedly increased NF-κB activity and MuRF1 transcriptional activation and is suppressed by genetic inactivation or biochemical suppression of MuRF1. In contrast, muscle wasting in PF mice is not affected by suppressing MuRF1. It remains to be determined if MuRF1 is expressed in the skeletal muscles of humans with ALI and whether blockade of MuRF1 could prevent muscle wasting in these patients. Although recognizing that the results obtained in the mouse may have limited relevance to ALI in humans, MuRF1 seems to be an attractive therapeutic target for ALI-associated skeletal muscle wasting.

Author disclosures are available with the text of this article at www.atsjournals.org.

Acknowledgment: The authors thank James Watkins and Andre Robinson in the Johns Hopkins Pulmonary Histology Core and the laboratory of Dr. Jeremy Walston for the use of their grip strength meter.

References

1. Ware LB, Matthay MA. The acute respiratory distress syndrome. *N Engl J Med* 2000;342:1334–1349.
2. Rubenfeld GD, Caldwell E, Peabody E, Weaver J, Martin DP, Neff M, Stern EJ, Hudson LD. Incidence and outcomes of acute lung injury. *N Engl J Med* 2005;353:1685–1693.
3. Ali NA, O'Brien JM Jr, Hoffmann SP, Phillips G, Garland A, Finley JC, Almoosa K, Hejal R, Wolf KM, Lemeshow S, *et al*; Midwest Critical Care Consortium. Acquired weakness, handgrip strength, and mortality in critically ill patients. *Am J Respir Crit Care Med* 2008;178:261–268.
4. Fletcher SN, Kennedy DD, Ghosh IR, Misra VP, Kiff K, Coakley JH, Hinds CJ. Persistent neuromuscular and neurophysiologic abnormalities in long-term survivors of prolonged critical illness. *Crit Care Med* 2003;31:1012–1016.
5. Herridge MS, Cheung AM, Tansey CM, Matte-Martyn A, Diaz-Granados N, Al-Saidi F, Cooper AB, Guest CB, Mazer CD, Mehta S, *et al.* Canadian Critical Care Trials Group One-year outcomes in survivors of the acute respiratory distress syndrome. *N Engl J Med* 2003;348:683–693.
6. Herridge MS, Tansey CM, Matté A, Tomlinson G, Diaz-Granados N, Cooper A, Guest CB, Mazer CD, Mehta S, Stewart TE, *et al*; Canadian Critical Care Trials Group. Functional disability 5 years after acute respiratory distress syndrome. *N Engl J Med* 2011;364:1293–1304.
7. De Jonghe B, Bastuji-Garin S, Durand MC, Malissin I, Rodrigues P, Cerf C, Outin H, Sharshar T. Groupe de Réflexion et d'Etude des Neuromyopathies en Réanimation. Respiratory weakness is associated with limb weakness and delayed weaning in critical illness. *Crit Care Med* 2007;35:2007–2015.
8. Sharshar T, Bastuji-Garin S, Stevens RD, Durand MC, Malissin I, Rodriguez P, Cerf C, Outin H, De Jonghe B. Presence and severity of intensive care unit- acquired paresis at time of awakening are associated with increased intensive care unit and hospital mortality. *Crit Care Med* 2009;37:3047–3053.
9. al-Lozi MT, Pestronk A, Yee WC, Flaris N, Cooper J. Rapidly evolving myopathy with myosin-deficient muscle fibers. *Ann Neurol* 1994;35:273–279.
10. Norman H, Zackrisson H, Hedstrom Y, Andersson P, Nordquist J, Eriksson LI, Libelius R, Larsson L. Myofibrillar protein and gene expression in acute quadriplegic myopathy. *J Neurol Sci* 2009;285:28–38.
11. Sher JH, Shafiq SA, Schutta HS. Acute myopathy with selective lysis of myosin filaments. *Neurology* 1979;29:100–106.
12. Bodine SC, Latres E, Baumhueter S, Lai VK, Nunez L, Clarke BA, Poueymirou WT, Panaro FJ, Na E, Dharmarajan K, *et al.* Identification of ubiquitin ligases required for skeletal muscle atrophy. *Science* 2001;294:1704–1708.
13. Gomes MD, Lecker SH, Jagoe RT, Navon A, Goldberg AL. Atrogin-1, a muscle- specific f-box protein highly expressed during muscle atrophy. *Proc Natl Acad Sci USA* 2001;98:14440–14445.
14. Doucet M, Russell A, Léger B, Debigaré R, Joanisse DR, Caron M, LeBlanc P, Maltais F. Muscle atrophy and hypertrophy signaling in patients with chronic obstructive pulmonary disease. *Am J Respir Crit Care Med* 2007;176:261–269.
15. Hussain SN, Mofarrahi M, Sigala I, Kim HC, Vassilakopoulos T, Maltais F, Bellenis I, Chaturvedi R, Gottfried SB, Metrakos P, *et al.* Mechanical ventilation-induced diaphragm disuse in humans triggers autophagy. *Am J Respir Crit Care Med* 2010;182:1377–1386.
16. D'Alessio FR, Tsushima K, Aggarwal NR, West EE, Willett MH, Britos MF, Pipeling MR, Brower RG, Tuder RM, McDyer JF, *et al.* Cd4+cd25+foxp3+ Tregs resolve experimental lung injury in mice and are present in humans with acute lung injury. *J Clin Invest* 2009; 119:2898–2913.
17. Files DC, DeGorordo A, Kesari P, Johnston L, Tsushima K, Aggarwal N, Sidhaye VK, D'Alessio F, King LS, Crow MT. Lung injury induces a skeletal muscle program that is qualitatively different from that induced by starvation. Oral presentation, ATS Annual Meeting, 2009, San Diego, CA.
18. Files DC, D'Alessio FR, Johnston L, Aggarwal NR, Garibaldi BT, Sidhaye VK, Chau E, Cohn R, King LS, Crow MT. Skeletal muscle atrophy in acute lung injury: differing mechanisms for wasting both during and after lung injury. Poster presentation, ATS Annual Meeting, 2010, New Orleans, LA.
19. Files DC, Johnston L, D'Alessio FR, Simmers J, Cohn RD, King L, Crow MT. Muscle RING-finger protein-1 (MuRF-1) is a critical mediator of acute lung injury-associated muscle wasting. Poster presentation, ATS Annual Meeting, 2011, Denver, CO.
20. Halbower AC, Mason RJ, Abman SH, Tuder RM. Agarose infiltration improves morphology of cryostat sections of lung. *Lab Invest* 1994;71: 149–153.
21. Whittemore LA, Song K, Li X, Aghajanian J, Davies M, Girgenrath S, Hill JJ, Jalenak M, Kelley P, Knight A, *et al.* Inhibition of myostatin

in adult mice increases skeletal muscle mass and strength. *Biochem Biophys Res Commun* 2003;300:965–971.

22. Mei SH, McCarter SD, Deng Y, Parker CH, Liles WC, Stewart DJ. Prevention of LPS-induced acute lung injury in mice by mesenchymal stem cells overexpressing angiopoietin 1. *PLoS Med* 2007;4:e269.
23. Rojas M, Woods CR, Mora AL, Xu J, Brigham KL. Endotoxin-induced lung injury in mice: structural, functional, and biochemical responses. *Am J Physiol Lung Cell Mol Physiol* 2005;288:L333–L341.
24. Cohen S, Brault JJ, Gygi SP, Glass DJ, Valenzuela DM, Gartner C, Latres E, Goldberg AL. During muscle atrophy, thick, but not thin, filament components are degraded by MuRF1-dependent ubiquitinylation. *J Cell Biol* 2009;185:1083–1095.
25. Dehoux MJ, van Beneden RP, Fernandez-Celemin L, Lause PL, Thissen JP. Induction of mafbx and MuRF ubiquitin ligase mRNAs in rat skeletal muscle after LPS injection. *FEBS Lett* 2003;544:214–217.
26. Lecker SH, Jagoe RT, Gilbert A, Gomes M, Baracos V, Bailey J, Price SR, Mitch WE, Goldberg AL. Multiple types of skeletal muscle atrophy involve a common program of changes in gene expression. *FASEB J* 2004;18:39–51.
27. Sachek JM, Hyatt JP, Raffaello A, Jagoe RT, Roy RR, Edgerton VR, Price SR, Mitch WE, Goldberg AL. Rapid disuse and denervation atrophy involve transcriptional changes similar to those of muscle wasting during systemic diseases. *FASEB J* 2007;21:140–155.
28. Waddell DS, Baehr LM, van der Brandt J, Johnsen SA, Reichart HM, Furlow JD, Bodine SC. The glucocorticoid receptor and FOX01 synergistically activate the skeletal muscle atrophy-associated MuRF1 gene. *Am J Physiol Endocrinol Metab* 2008;285:E785–E797.
29. Acharyya S, Guttridge DC. Cancer cachexia signaling pathways continue to emerge yet much still points to the proteasome. *Clin Cancer Res* 2007;13:1356–1361.
30. Reed SA, Senf SM, Cornwell EW, Kandarian SC, Judge AR. Inhibition of IkappaB kinase alpa (IKKα) or IKKbeta (IKKβ) plus Forkhead box O (Foxo) abolishes skeletal muscle atrophy. *Biochem Biophys Res Commun* 2011;405:491–496.
31. Cai D, Frantz JD, Tawa NE Jr, Medendez PA, Oh BC, Lidov HG, Hasselgren PO, Frontera WR, Lee J, Glass DJ, *et al*. IKKbeta/NF-kappaB activation causes severe muscle wasting in mice. *Cell* 2004; 119:285–298.
32. Moriscot AS, Baptista IL, Bogomolovas J, Witt C, Nirner S, Granzier H, Labeit S. MuRF1 is a muscle fiber type-II associated factor and together with MuRF2 regulates type II fiber trophicity and maintenance. *J Struct Biol* 2010;170:344–353.
33. Masiero E, Agatea L, Mammucari C, Blaauw B, Loro E, Komatsu M, Metzger D, Reggiani C, Schiaffino S, Sandri M. Autophagy is required to maintain muscle mass. *Cell Metab* 2009;10:507–515.
34. Komatsu M, Ichimura Y. Physiological significance of selective degradation of p62 by autophagy. *FEBS Lett* 2010;584:1374–1378.
35. Morris PE, Goad A, Thompson C, Taylor K, Harry B, Passmore L, Ross A, Anderson L, Baker S, Sanchez M, *et al*. Early intensive care unit mobility therapy in the treatment of acute respiratory failure. *Crit Care Med* 2008;36:2238–2243.